AN INHOMOGENEOUS JET MODEL FOR THE RAPID VARIABILITY OF TeV BLAZARS

BOUTELIER T.[1], HENRI G.[1], PETRUCCI P.O.[1]
[1]Laboratoire d'Astrophysique de Grenoble - Université Joseph-Fourier/CNRS UMR 5571 - BP 53, F-38041 Grenoble, France

ABSTRACT: We present a new time-dependent inhomogeneous jet model of non-thermal blazar emission, which reproduces the entire spectral energy distribution together with the rapid gamma-ray variability. Ultra-relativistic leptons are injected at the base of a jet and propagate along the jet structure. We assume continuous reacceleration and cooling, producing a relativistic quasi-maxwellian (or "pile-up") particle energy distribution. The synchrotron and Synchrotron-Self Compton jet emissivity are computed at each altitude. Klein-Nishina effects as well as intrinsic gamma-gamma absorption are included in the computation. Due to the pair production optical depth, considerable particle density enhancement can occur, particularly during flaring states.Time-dependent jet emission can be computed by varying the particle injection, but due to the sensitivity of pair production process, only small variations of the injected density are required during the flares. The stratification of the jet emission, together with a pile-up distribution, allows significantly lower bulk Lorentz factors, compared to the ones obtained with the commonly used one-zone models, in better agreement with observational and statistical constraints. Applying this model to the case of PKS 2155-304 and its big TeV flare observed in 2006, we can reproduce simultaneously the average broad band spectrum of this source as well as the TeV spectra and TeV light curve of the flare with bulk Lorentz factor lower than 15.

INTRODUCTION: The blazar phenomenon is due to relativistic Doppler boosting of the non-thermal jet emission taking place in radio-loud Active Galactic Nuclei (AGN) whose jet axis is closely aligned with the observer's line of sight. Blazars exhibit a spectral energy distributions (SED) dominated by two broad band components. In the Synchrotron Self Compton scenario (SSC), the lowest energy hump is attributed to the synchrotron emission of relativistic leptonic particles, and the highest one is attributed to the Inverse Compton process (IC) of the same leptons on the synchrotron photon field.

These objects are highly variable at all wavelength. The most extreme example of this variability behaviour has been caught by the H.E.S.S. instrument in the recent observations of PKS 2155-304 during summer 2006 (Aharonian et al. 2007 see also Albert et al. 2007 for the case of Mrk 501).

Case of PKS 2155-304 "big flare":

Tvar ~200 sec ⇒ Γ_b> 50 for 1 zone homogeneous models(Begelman et al. 2007).

But:

➡High bulk Lorentz factor in contradiction with constrains derived from other observational evidence (Henri & Saugé 2006).

➡One-zone models unable to fit the entire spectrum, the low energy radio points being generally attributed to more distant emitting regions.

Objectives:

We present a new approach, unifying small and large scales emission regions: we consider that the radio jet is filled by the same particles originating from the high energy emitting region (bottom of the jet), that have propagated along it. We describe the emitting plasma by a continuous and variable particle injection, submitted to continuous reacceleration and radiative cooling. This model fits into the two-flow framework originally proposed by Pelletier (1985) and Sol et al. (1989), where a non relativistic, but powerful MHD jet launched by the accretion disk, surrounds a highly relativistic plasma of electron-positron pairs propagating along its axis. The MHD jet plays the role of a collimater and an energy reservoir for the pair plasma, which is responsible for the observed broad band emission. We show an application to the case of PKS 2155-304, focusing on the 2006 big flare event.

DESCRIPTION OF THE MODEL:

Geometry:

The pair plasma propagates in a stationary funnel whose geometry is parametrized as:

$$\mathbf{r(z) = R_0\left[\frac{z}{Z_0}+\left(\frac{R_i}{R_0}\right)^{1/\omega}\right]^{\omega}}$$

The magnetic field has the following dependency:

$$\mathbf{B(z) = B_0\left(\frac{r(z)}{R_0}\right)^{-\lambda}}$$

The plasma accelerates in the jets on a typical length Z_0, and the bulk Lorentz factor fallows:

$$\mathbf{\Gamma_b(z) = \left[1+\frac{\Gamma_{b\infty}^a-1}{1+\frac{z_0}{z}}\right]^{1/a}}$$

Particule energy distribution (EDF):

A second order acceleration process carry energy from the magnetic turbulence of the MHD jet to

$$\mathbf{n(\gamma,z,t) = n_0(z,t)\gamma^2\exp\left(-\frac{\gamma}{\gamma_0(z,t)}\right)}$$

the plasma beam. The EDF is a relativistic maxwellian (pile-up):

Particles loose energy via synchrotron and inverse Compton cooling. A fast reacceleration process heat the particle as they propagate in the jet. The acceleration rate is parametrized as a shifted

$$\mathbf{Q_{acc}(z) = Q_0\left[\frac{z}{Z_0}+\left(\frac{R_i}{R_0}\right)^{1/\omega}\right]^{-\zeta}\exp\left(-\frac{z}{Z_c}\right)}$$

power law, with an exponential cut-off at the altitude Z_c:

By balancing the acceleration rate and the losses term, we compute the characteristic Lorentz factor of the pile-up distribution at each altitude z

Pair production:

We compute at each altitude the pair production optical depth. The absorbed gamma-ray photons

$$\mathbf{\Phi(z,t) = \int n(\gamma,z,t)S(z)\Gamma_b\beta_b c\,d\gamma}$$

$\Phi(z,t)$lead to new pairs that are continuously reaccelerated. The particle flux increase in the jet: is computed through a continuity equation. It's variations measure the importance of pair creation (see Fig. 4).

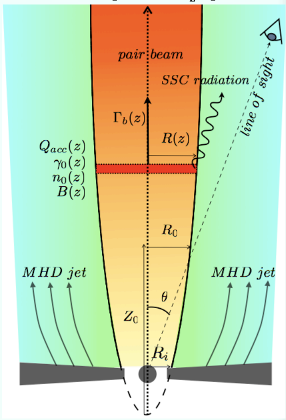

Figure 1: *Sketch of the jet geometry*

Jet $\mathbf{n_0(z,t),\ \gamma_0(z,t),\ r(z,t)}$ and $\mathbf{B(z,t)}$,***spectrum:***

Knowing the emissivity is computed at each altitude in the jet, assuming a SSC process for the radiative mechanism. The total intensity is

$$\mathbf{I_\nu(t) = \int_{jet}\left(j_\nu^{SYN}(z,t)+j_\nu^{CI}(z,t)\right)dSdz}$$

determined by integrating the emissivity along the jet:

The emissivity is enhanced in the observer frame by the Doppler boosting, and we take into account the attenuation factor of the gamma ray signal by the cosmic diffuse infrared background, chosen as the modified Primack model P45 (Aharonian et al. 2006).

To obtain time dependent solutions, all parameters remain fixed except the particle injection rate and/or the acceleration rate that are adjusted to fit observed data. The variability time scale is: $\mathbf{t_{var} \simeq \frac{Z_0}{c}(1-\beta_b\cos\theta) = \frac{Z_0}{c\Gamma_b\delta}}$

TIME DEPENDENT SIMULATIONS AND APPLICATIONS TO PKS 2155-304:

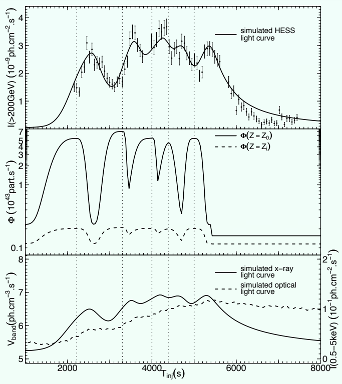

Figure 2: ***Upper panel****: H.E.S.S. light curve above 200 GeV superimposed with the model (solid line).* ***Middle panel****: time dependent particle injection function used in the simulation.* ***Lower panel****: predicted light curves in X-ray (dashed line, left y-scale) and optical (dot-dashed line, right y-scale). The dotted lines mark the maximum of the different bursts of the injection function.*

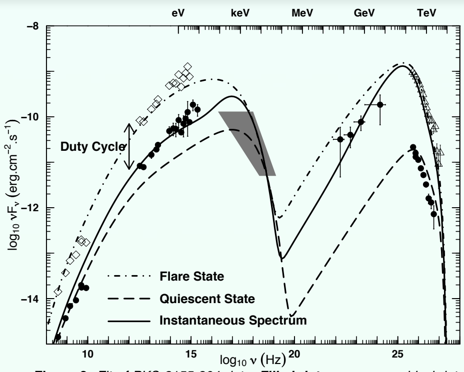

Figure 3: *Fit of PKS 2155-304 data.* ***Filled dots****: average archival data.* ***Empty triangles****: average HESS data from the big flaring night.* ***Empty diamonds****: "fake flaring" state low energy points with a duty cycle f=0.1 (see text).* ***Shaded area****: envelopppe of archival X-ray data from BeppoSAX, SWIFT and XMM-Newton.* ***Dot-dashed line****: best fit of the " average fake flaring" spectrum.* ***Dashed line****: fit of the quiescent (~average) spectrum.* ***Solid line****: example of an instantaneous simulated spectrum.*

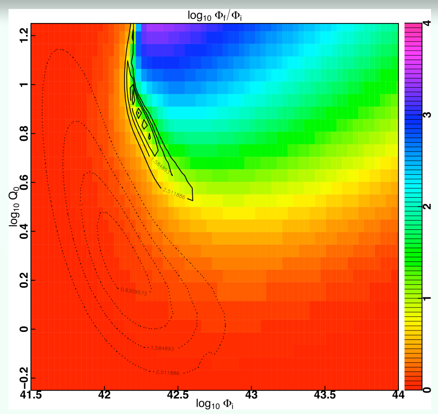

Figure 4: *The color scale represents the decimal logarithm of the ratio between the particule flux at the base of the jet and at the end of the jet, depending on the acceleration rate and the injected flux of particule.* ***Solid lines****: χ^2 contours for the flaring state.* ***Dashed lines****: χ^2 contours for the stationary state.*

STATE		$\Phi(Z_i)$ [$10^{42}s^{-1}$]	$\Phi(Z_0)$ [$10^{42}s^{-1}$]	Q_0 [s^{-1}]	$\Gamma_{b\infty}$	R_i [$10^{14}cm$]	R_0 [$10^{14}cm$]	Z_0 [$10^{15}cm$]	Z_c [$10^{21}cm$]	B_0 [G]	ω	λ	ζ
flaring	Max	2.09	70.1										
	Aver.	1.84	24.4	6.5	15	1.1	1.78	2	5	5	0.2	1.9	1.27
	Min	1.16	2.33										
quiescent		1.16	1.55	2.5									

Table 1: *Model parameters of the flaring and quiescent state. During the flaring state, the flux of injected particles varies between the indicated minimum and maximum values, the other parameters remain fixed.*

Method:

1.We construct a "fake flaring" spectrum, that would be observed in case the object was continuously flaring. The low energy data are multiplied by a factor *f* to take into account that the object is flaring with the duty cyle *1/f.*

2.We fit the fake flaring spectrum (stationary) and derive the model parameters.

3.Letting only the particle injection rate and the acceleration rate free to vary, we fit the quiescent state.

4.To fit the flaring episod of PKS 2155-304, we let only the particle injection rate free to vary, $N_0(t)$. The injection function is a succession of 5 assymetric gaussians, as used in the light curve analysis from Aharonian et al. (2007).

The fit parameters are given in Table 1.

Results:

•Our model success to reproduce the entire broad band spectrum of PKS 2155-304 in the flaring state (Fig. 3), as well as the observed H.E.S.S. light curve (Fig. 2).

•The data are fitted with a bulk Lorentz factor of 15. The use of a pile-up distribution (low local soft photons density), and of a jet geometry (gamma-rays and soft photons not emitted cospatially), relaxes strongly the constrains on opacity.

•The middle panel of Fig. 2 shows that the flaring states is caracterized by a strong pair creation, and a high sensitivity of initial conditions. A small variation of the injected particule rate leads to strong variations in the TeV light curve.

•As shown on Fig. 4, the transition between quiescent and flaring state is compatible with an increase of the acceleration rate. The flaring state is accompanied by high creation pair, and by a high sensitivity to the initial conditions (see middle panel of Fig. 2).

REFERENCES:

•Aharonian F., et al., 2007, ApJL, 664, L71
•Aharonian F., et al., 2006, Nature, 440, 1018
•Albert J., et al., 2007, ApJ, 669, 862
•Begelman M. C., Fabian A. C., Rees M. J., 2008, MNRAS,
•384, L19
•Henri G., Saugé L., 2006, ApJ, 640, 185
•Pelletier G., 1985, in Plasma turbulence and Astrophysical Objects, Société Française de Physique (SFP)
•Sol H., Pelletier G., Asseo E., 1989, MNRAS, 237, 411

Acknowledgements:
The sponsorship of ESA and ESA Education in providing financial support to attend to The 2008 X-ray Universe conference is gratefully acknowledged by the authors.